

Phase-Field modeling of brittle fracture of orthotropic materials

Diego Dias Velo
Ayrton Ribeiro Ferreira (Prof. Dr.) (Advisor)

Departamento de Engenharia de Estruturas
Escola de Engenharia de São Carlos
Universidade de São Paulo

November 10, 2025

Topics

1 Introduction

- Importance of Fracture Mechanics
- Anisotropic Fracture

2 Objectives

- Novel Contributions
- Schedule

3 State of the Art

- Griffith Theory
- Phase-Field Method
- Gradient Split

4 Computational Implementation

- High-Performance Computing Tools
- Global Minimization
- Linear Momentum Solution
- Damage Solution

5 Results

Topics (cont.)

- Single Edge Notch Mode I
- Single Edge Notch Mode II
- L-Shaped Specimen
- Holed Plate Specimen

6 Partial Conclusions

- Results and Discussion
- Limitations and Future Work

7 Next Steps

- Fracture Toughness Anisotropy

8 References and Acknowledgments

Introduction

Importance of Fracture Mechanics

The importance of fracture mechanics can be summarized as follows:

- **Safety:** Predicting failure modes helps prevent catastrophic failures in structures such as bridges, buildings, and aircraft.
 - **Material Design:** Insights from fracture mechanics guide the development of new materials with improved toughness and durability.

Anisotropic Materials

The importance of anisotropic fracture mechanics include:

- **Directional Dependence** : Many engineering materials exhibit anisotropic properties.

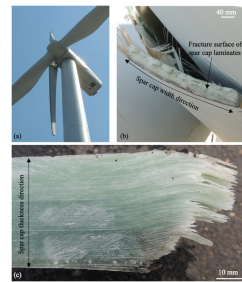
Figure: Examples of anisotropic materials.



(a) Military Aircrafts



(b) Jet Engine Turbo Blade



(c) Wind Turbine

Source: Wikipedia.

Objectives

Expected Contributions

The main contributions of this work are:

- **Extend the Ferreira, Marengo e Perego (2024) phase-field model to anisotropic materials.**
- **Implementation of a FEM code on top of HPC techniques.**
- **Validation of the model for orthotropic materials.**
- **Couple the elastic and fracture toughness anisotropies on the fracture process.**

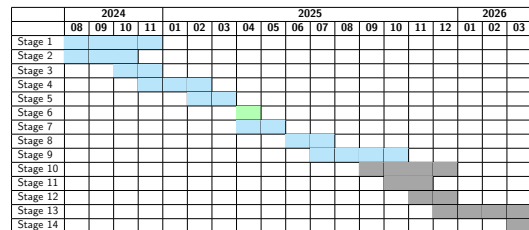
Schedule

Table: Activities to be developed.

No.	Activity description
01	complete the mandatory course credits for the master's program
02	bibliographic review
03	study parallelization libraries: PETSc and ParMETIS
04	implementation of the classical isotropic model of Bourdin, Francfort e Marigo (2000)
05	writing the qualification document
06	qualification exam
07	implementation of the energy decomposition of Ferreira, Marengo e Perego (2024)
08	formulation and implementation of the anisotropic elastic constitutive model
09	formulation and implementation of anisotropic fracture resistance
10	period at the Polytechnic University of Milan, Italy
11	development of numerical examples
12	writing a scientific article for an international journal
13	writing the thesis document
14	defense

Authors.

Table: Activites Timeline.



Authors.

State of the Art

Griffith Theory

$$\Pi = U_{elastic} + \textcolor{red}{U_{plastic}} + U_{fracture} - W_{ext} \quad \xrightarrow{\text{Brittle}} \quad \dot{\Pi} = \dot{U}_{elastic} + \dot{U}_{fracture} - \dot{W}_{ext} \quad (1)$$

For a closed system, $\dot{\Pi} = 0$, then the **dissipation** Φ is

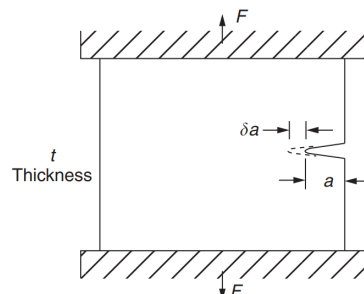
$$\Phi = \dot{W}_{ext} - \dot{U}_{elastic} := G\dot{a} = -\frac{d\Pi}{da}\dot{a} \quad , \quad G = -\frac{d\Pi}{da}$$

and Griffith's criterion becomes

$$G \geq G_c \quad , \text{and} \quad \begin{cases} \dot{a} > 0 \rightarrow G = G_c \\ \dot{a} = 0 \rightarrow G < G_c \end{cases} \quad (2)$$

Critical length of a crack, a_c , is given by $a_c = \frac{2EG_c}{\pi\sigma^2}$.

Figure: Body undergoing fracture.



Jones e Ashby (2019).

Phase-Field Method

The variational recast done by Francfort e Marigo (1998)

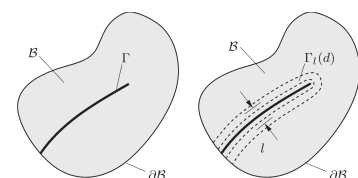
$$\Pi_{int} = \underbrace{\int_{\Omega} \psi(\varepsilon) d\Omega}_{\text{Elastic}} + \underbrace{\int_{\Gamma} G_c dA}_{\text{Dissipation}} . \quad (3)$$

and its regularization by a phase-field d performed by Bourdin, Francfort e Marigo (2000)

$$\Pi_{int} = \int_{\Omega} \psi(\varepsilon, \mathbf{d}) d\Omega + \int_{\Omega} \varphi(\mathbf{d}, \nabla \mathbf{d}) d\Omega . \quad (4)$$

$$\begin{cases} \psi(\varepsilon, d) = \omega(d)\psi_0(\varepsilon) \\ \varphi(d, \nabla d) = G_c [w(d) + c_d |\nabla d|^2] \end{cases} \quad (5)$$

Figure: (a) Sharp crack surface Γ and (b) the regularized crack region Γ_l .



Miehe, Hofacker e Welschinger (2010)

Phase-Field Method

The Strain and dissipation energy densities

$$\psi(\boldsymbol{\varepsilon}, d) = \omega(d) \psi_0(\boldsymbol{\varepsilon}), \quad \omega(d) = (1 - d)^2$$

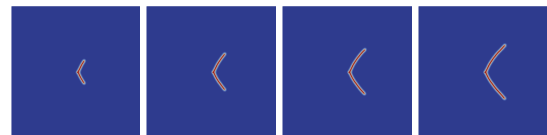
$$\varphi(d, \nabla d) = G_c [w(d) + c_d |\nabla d|^2]$$

where

$$w(d) = \begin{cases} \frac{3}{8l_0}d & \text{AT1} \\ \frac{1}{2l_0}d^2 & \text{AT2} \end{cases}$$

$$c_d = \begin{cases} \frac{3}{8}l_0 & \text{AT1} \\ \frac{1}{2}l_0 & \text{AT2} \end{cases}$$

Figure: Interpenetration due to symmetric degradation.



Source: Authors.

Assymmetric degradation of the strain energy

$$\psi(\boldsymbol{\varepsilon}, d) = \omega(d)\psi_0^+(\boldsymbol{\varepsilon}) + \psi_0^-(\boldsymbol{\varepsilon})$$

Volumetric-Deviatoric Split

$$\psi_0^\pm(\boldsymbol{\varepsilon}) = H^\pm(\text{Tr}(\boldsymbol{\varepsilon})) \frac{\kappa}{2} (\text{Tr}(\boldsymbol{\varepsilon}))^2 + \mu \boldsymbol{\varepsilon}_D : \boldsymbol{\varepsilon}_D \quad (6)$$

Gradient Energy Split

$$\psi(\varepsilon, d) = \int_{\Omega} [\omega(d) + [1 - \omega(d)] H^-(\sigma_{0n})] \psi_0(\varepsilon) d\Omega \quad , \quad (7)$$

where

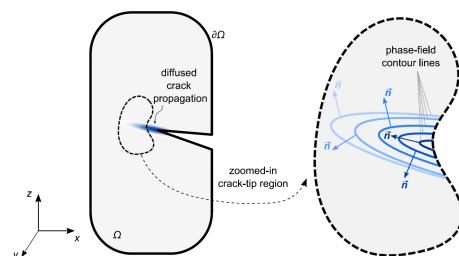
$$\sigma_{0n} \equiv \sigma : n \otimes n \quad . \quad (8)$$

and the projection direction is given by

$$\mathbf{n} := \begin{cases} -\frac{\nabla d}{\|\nabla d\|} & \text{if } \nabla d \neq 0 \\ \mathbf{0} & \text{if } \nabla d = 0 \end{cases} \quad (9)$$

$$\sigma_{0n} := \begin{cases} \sigma : n \otimes n & \text{if } \nabla d \neq 0 \\ \text{Tr}(\sigma) & \text{if } \nabla d = 0 \end{cases} \quad (10)$$

Figure: Normal to crack direction.



Ferreira, Marengo e Perego (2024)

Computational Implementation

High-Performance Computing Tools

The following high-performance computing tools are utilized in the implementation:

- **PETSc**: A suite of data structures and routines for the scalable (parallel) solution of scientific applications modeled by partial differential equations.
- **METIS**: A software package for partitioning unstructured graphs and computing fill-reducing orderings of sparse matrices.
- **GMSH**: A 3D finite element mesh generator with built-in pre- and post-processing facilities.
- **HDF5**: A data model, library, and file format for storing, managing and built for fast I/O processing and storage.
- **Paraview**: An open-source, multi-platform data analysis and visualization application.

PETSc

PETSc (Portable, Extensible Toolkit for Scientific Computation) is designed for the **scalable** solution of scientific applications modeled by partial differential equations (**PDEs**).



It is a powerful and convenient interface for:

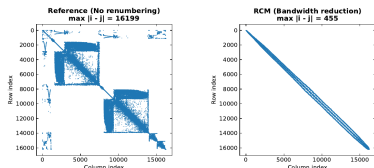
- Management of **parallelism and communication**.
- **Algebraic operations** on distributed vectors (Vec) and matrices(Mat).
- Linear (KSP) and nonlinear (SNES) **solvers** (algorithms (NR, LS, TR, etc) based on KSP objects).

METIS

METIS is a library for partitioning and producing fill reducing orderings for finite element meshes.

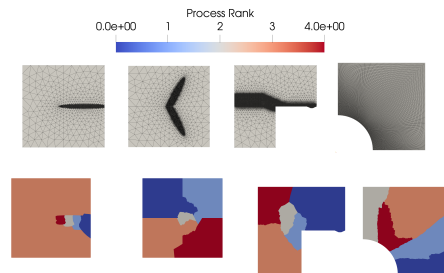
- **Fill-reducing:** METIS_NodeND.
- **Mesh Partitioning:** METIS_PartMeshDual.

Figure: Sparse matrix representation.



Authors.

Figure: Mesh partitioning.



Authors.

C++, HDF5, Paraview, GMSH, Python

- **C++**: The programming language used for the implementation.
- **HDF5**: Built for fast I/O processing and storage.
- **Paraview**: Open-source multiple-platform application for interactive, scientific visualization.
- **GMSH**: A 3D finite element mesh generator with built-in pre- and post-processing facilities.
- **Python**: A programming language used for pre- and post-processing and for the GMSH API.



Paraview



Solution of the coupled problem

- **Monolithic approach** (BHARALI et al., 2022)

$$\begin{bmatrix} \mathbf{K}^{uu} & \mathbf{K}^{ud} \\ \mathbf{K}^{du} & \mathbf{K}^{dd} \end{bmatrix} \begin{bmatrix} \Delta \mathbf{u} \\ \Delta d \end{bmatrix} = \begin{bmatrix} \mathbf{r}^u \\ \mathbf{r}^d \end{bmatrix} \quad (11)$$

- **Staggered approach**

$$\begin{bmatrix} \mathbf{K}^{uu} & 0 \\ 0 & \mathbf{K}^{dd} \end{bmatrix} \begin{bmatrix} \Delta \mathbf{u} \\ \Delta d \end{bmatrix} = \begin{bmatrix} \mathbf{r}^u \\ \mathbf{r}^d \end{bmatrix} \quad (12)$$

or, in more detail,

$$\begin{cases} \partial_u \Pi_{n+1}(\mathbf{u}_{n+1}^{i+1}, d_{n+1}^i) = 0 \\ \partial_d \Pi_{n+1}(\mathbf{u}_{n+1}^{i+1}, d_{n+1}^{i+1}) [\Delta d_{n+1}^{i+1}] = 0, \quad \partial_d \Pi_{n+1}(\mathbf{u}_{n+1}^{i+1}, d_{n+1}^{i+1}) \geq 0, \quad \Delta d_{n+1}^{i+1} \geq 0 \end{cases} \quad . \quad (13)$$

Staggered approach

Require: Load solution (\mathbf{u}_n, d_n) from step n and boundary conditions g_{n+1}, t_n at current step n

- 1: initialize $i \leftarrow 0$
- 2: set $(\mathbf{u}^0, d^0) \leftarrow (\mathbf{u}_n, d_n)$
- 3: **while** $Re_{\text{stag}} \geq TOL_{\text{stag}}$ **do**
- 4: $i \leftarrow i + 1$
- 5: given $d^{i-1} = d_n + \Delta d^{i-1}$, find \mathbf{u}^i solving $\partial_{\mathbf{u}} \Pi_{n+1}(\mathbf{u}^i, d^{i-1}) = 0$
- 6: given \mathbf{u}^i , find Δd^i solving $\partial_d \Pi_{n+1}(u^i, d_n)[\Delta d^i] = 0$ with $\partial_d \Pi_{n+1}(\mathbf{u}^i, d_n) \geq 0$, $\Delta d^i \geq 0$
- 7: compute $|Re_{\text{stag}} = \partial_{\mathbf{u}} \Pi_{n+1}(\mathbf{u}^i, d^i)[\Delta \mathbf{u}^i]|$
- 8: **end while**
- 9: $(\mathbf{u}_{n+1}, d_{n+1}) \leftarrow (\mathbf{u}^i, d^i)$

Linear Momentum Solution

From Principle of Virtual Work, the weak form is given as:

$$\int_{\Omega} [\nabla^s \mathbf{w} : \mathbb{D} \nabla^s \mathbf{u}] dV = \int_{\Gamma_t} \mathbf{t} \cdot \mathbf{w} dS + \int_{\mathcal{B}} \mathbf{b} \cdot \mathbf{w} dV \quad \forall \mathbf{w} = 0 \text{ on } \Gamma_u \quad (14)$$

$$\begin{cases} \mathbf{u}(x, y) = \mathbf{N}^e(x, y) \mathbf{u}^e \\ \mathbf{w}(x, y) = \mathbf{N}^e(x, y) \mathbf{w}^e \end{cases} \quad \forall (x, y) \in \Omega_e \quad (15)$$

$$\boldsymbol{\varepsilon} = \nabla^s \mathbf{u} = \mathbf{B}^e \mathbf{u}^e \quad (16)$$

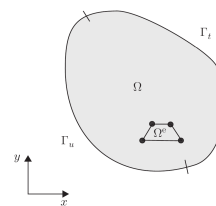
and the system of equations can be written as

$$\mathbf{K} \mathbf{u} = \mathbf{F} \quad (17)$$

where

$$\mathbf{K} = \sum_{e=1}^n \left[\int_{\Omega_e} \mathbf{B}_e^T \mathbb{C} \mathbf{B}_e d\Omega \right] \mathbf{u}^e \quad \text{and} \quad \mathbf{F} = \sum_{e=1}^n \int_{\Gamma_e} \mathbf{N}_e^T \mathbf{t} d\Gamma + \sum_{e=1}^n \int_{\Omega_e} \mathbf{N}_e^T \mathbf{b} d\Omega \quad (18)$$

Figure: Discrete domain.



Anand e Govindjee (2020).

Newton Raphson

Taylor expansion gives

$$\mathbf{R}(\mathbf{u}^{k+1}) = \mathbf{R}(\mathbf{u}^k) + \left[\frac{\partial \mathbf{R}}{\partial \mathbf{u}} \right]_{\mathbf{u}^k} (\mathbf{u}^{k+1} - \mathbf{u}^k) + \mathcal{O}\left(\left(\mathbf{u}^{k+1} - \mathbf{u}^k\right)^2\right) \quad (19)$$

that, after linearization and assuming that $\mathbf{R}(\mathbf{u}^{k+1}) = 0$

$$\mathbf{R}(\mathbf{u}^k) + \left[\frac{\partial \mathbf{R}}{\partial \mathbf{u}} \right]_{\mathbf{u}^k} (\mathbf{u}^{k+1} - \mathbf{u}^k) = 0 \quad , \quad (20)$$

Rearranging the equation, we can write

$$\left[\frac{\partial^2 \Pi}{\partial \mathbf{u}^2} \right]_{\mathbf{u}^k} \Delta \mathbf{u}^{k+1} = -\mathbf{R}(\mathbf{u}^k) \quad \Rightarrow \quad \mathbf{K}(\mathbf{u}^k) \Delta \mathbf{u}^{k+1} = -\mathbf{R}(\mathbf{u}^k) \quad (21)$$

PCFactorSetReuseOrdering(PETSC_TRUE) and KSPSetReusePreconditioner(PETSC_FALSE)

Line Search

Optimal step size

$$\mathbf{u}_n^{k+1} = \mathbf{u}^k + \eta_n \Delta \mathbf{u}^{k+1} \quad . \quad (22)$$

assuming that $\mathbf{R}(\eta_n) \perp \Delta \mathbf{u}$

$$\mathbf{R}(\eta_n) = \mathbf{R}(\eta_n) \cdot \Delta \mathbf{u} = \mathbf{R}(\mathbf{u}^k + \eta_n \Delta \mathbf{u}) \cdot \Delta \mathbf{u} \quad (23)$$

that, after some algebra, leads to the following iterative formula for η :

$$\eta_{n+1} = \begin{cases} \frac{\alpha_n}{2} + \sqrt{\left(\frac{\alpha_n}{2}\right)^2 - \alpha_n} & \text{if } \alpha_n < 0 \\ \frac{\alpha_n}{2} & \text{if } \alpha_n > 0 \end{cases} \rightarrow \text{where } \alpha_n = \frac{\mathbf{R}(\mathbf{u}^k)}{\mathbf{R}(\eta_n)} = \frac{R_0}{R(\eta_n)} \quad (24)$$

with a stopping criterion defined by Bonet, Gil e Wood (2016) as

$$|\mathbf{R}(\eta_n)| < \rho |\mathbf{R}(0)| \quad , \quad \text{which } \rho = 0.5 \quad (25)$$

Symmetric Linear Complementarity Problem (SLCP)

Marengo et al. (2021) performs a Taylor expansion around $\hat{\mathbf{d}}_n$

$$\Pi_{n+1}(\hat{\mathbf{u}}^i, \hat{\mathbf{d}}) = \underbrace{\frac{1}{2} \Delta \hat{\mathbf{d}}^\top Q^i \Delta \hat{\mathbf{d}} + \Delta \hat{\mathbf{d}}^\top q^i}_{\text{Term to be minimized}} + \Pi_{n+1}(\hat{\mathbf{u}}^i, \hat{\mathbf{d}}_n), \quad (26)$$

where

$$\Delta \hat{\mathbf{d}} = \hat{\mathbf{d}} - \hat{\mathbf{d}}_n, \quad Q^i = \nabla_{\hat{\mathbf{d}} \hat{\mathbf{d}}}^2 \Pi_{n+1}(\hat{\mathbf{u}}^i, \hat{\mathbf{d}}_n), \quad q^i = \nabla_{\hat{\mathbf{d}}} \Pi_{n+1}(\hat{\mathbf{u}}^i, \hat{\mathbf{d}}_n). \quad (27)$$

and finally, the Jacobian (Hessian) Q^i and Gradient(Residue) q^i are given by

$$Q^i := \Psi_e(\hat{\mathbf{u}}^i) + G_c \Phi_e, \quad q^i := Q^i \hat{\mathbf{d}}_n - \psi_e(\hat{\mathbf{u}}^i). \quad (28)$$

Symmetric Linear Complementarity Problem (SLCP)

Where, the constant element dissipation matrix Φ_e is given by

$$\Phi_e := \begin{cases} \int_{\Omega_e} \left(\frac{3l_0}{8} B_{d,e}^T B_{d,e} \right) d\Omega_e & \text{if AT1} \\ \int_{\Omega_e} \left(l_0^{-1} N_{d,e}^T N_{d,e} + l_0 B_{d,e}^T B_{d,e} \right) d\Omega_e & \text{if AT2} \end{cases} \quad (29)$$

and the element free energy matrix Ψ_e and vector ψ_e are given by

$$\Psi_e(\hat{\mathbf{u}}_e^i) := \int_{\Omega_e} 2 \psi_0^+(\hat{\mathbf{u}}_e^i) N_{d,e}^T N_{d,e} d\Omega_e \quad (30)$$

$$\psi_e(\hat{\mathbf{u}}_e^i) := \begin{cases} \int_{\Omega_e} \left[2 \psi_0^+(\hat{\mathbf{u}}_e^i) - \frac{3l_0}{8} \right] N_{d,e}^T d\Omega_e. & \text{if AT1} \\ \int_{\Omega_e} 2 \psi_0^+(\hat{\mathbf{u}}_e^i) N_{d,e}^T d\Omega_e. & \text{if AT2} \end{cases} \quad (31)$$

Projected Successive Over-Relaxation (PSOR)

The SLCP is gives rise to the following conditions:

$$\partial_d \Pi_{n+1}(\mathbf{u}_{n+1}, d_{n+1}) [\Delta d_{n+1}], \quad \partial_d \Pi_{n+1}(\mathbf{u}_{n+1}, d_{n+1}) \geq 0, \quad \Delta d_{n+1} \geq 0 \quad (32)$$

which can be solved by a Projected Successive Over-Relaxation (PSOR) iterative scheme

$$x^{k+1} = (\mathbf{L} + \mathbf{D})^{-1} (b - \mathbf{U}x^k) \quad (33)$$

which, after some algebra, Marengo et al. (2021) shows that can be written as

$$\Delta d_r^k = \left\langle \Delta d_r^{k-1} - D_{rr}^{-1} \left[Q_{rc} \Delta d_c^{k-1} + L_{rc} (\Delta d_c^k - \Delta d_c^{k-1}) \right] \right\rangle_+ \quad (34)$$

where

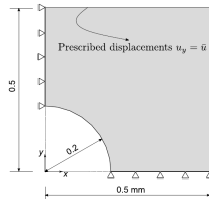
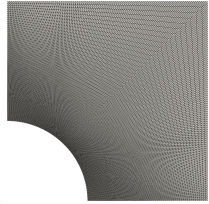
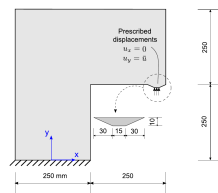
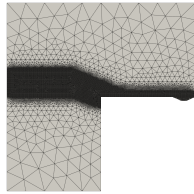
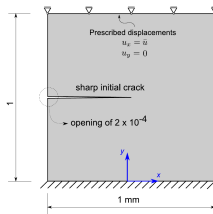
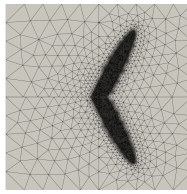
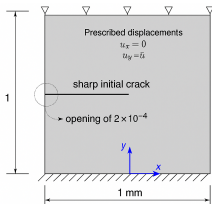
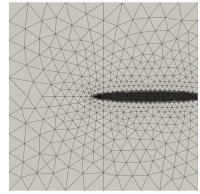
$$\begin{cases} L_{rc} := Q_{r>c} \\ D_{rr} := Q_{r=r} \end{cases} \quad (35)$$

$$\langle x \rangle_+ := \begin{cases} x & \text{if } x \geq 0 \\ 0 & \text{if } x < 0 \end{cases} \quad (36)$$

Results

Physical Properties for Benchmark Examples

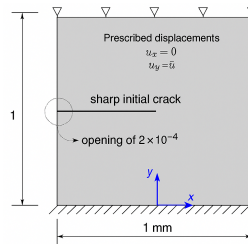
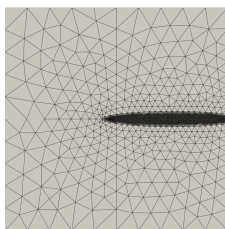
Figure: Benchmarks.



Authors.

Single Edge Notch Mode I

Figure: Geometry and boundary conditions.



Imposed cyclic displacement

$$\Delta \bar{u}_n = \begin{cases} 4 \times 10^{-3} \text{ mm} & \text{if } 1 \leq n \leq 20 \\ -4 \times 10^{-4} \text{ mm} & \text{if } 21 \leq n \leq 60 \\ 4 \times 10^{-4} \text{ mm} & \text{if } 61 \leq n \leq 80 \end{cases}$$

Source: Ferreira, Marengo e Perego (2024).

Table: Physical properties for benchmark examples.

Example	E GPa	ν	G_c N/mm	ℓ_0 mm
SEN Mode I	210	0.3	2.7	0.01

Source: Authors.

Figure: Specimen with load reversal.



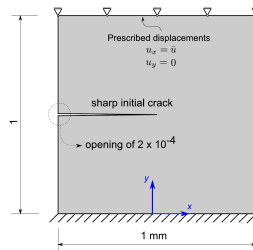
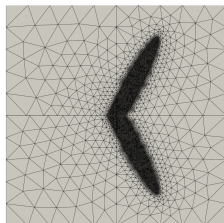
Figure: Reaction forces.

Source: Authors.

Source: Authors.

Single Edge Notch Mode II

Figure: Geometry and boundary conditions.



The imposed cyclic loading for this case is:

$$\Delta \bar{u}_n = \begin{cases} 1 \times 10^{-3} \text{ mm} & \text{if } 1 \leq n \leq 6 \\ 3 \times 10^{-4} \text{ mm} & \text{if } 7 \leq n \leq 26 \\ -3 \times 10^{-4} \text{ mm} & \text{if } 27 \leq n \leq 106 \\ 3 \times 10^{-4} \text{ mm} & \text{if } 107 \leq n \leq 146 \end{cases}$$

Source: Ferreira, Marengo e Perego (2024).

Table: Physical properties for benchmark examples.

Example	E GPa	ν	G_c N/mm	ℓ_0 mm
SEN Mode II	210	0.3	2.7	0.01

Source: Authors.

Figure: Specimen with load reversal.



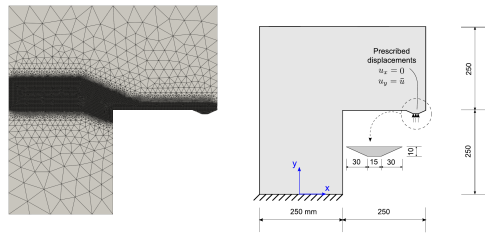
Figure: Reaction forces.

Source: Authors.

Source: Authors.

L-Shaped Specimen

Figure: Geometry and boundary conditions.



Subjected to the following displacement history:

$$\Delta \bar{u}_n = \begin{cases} 1 \times 10^{-2} \text{ mm} & \text{if } 1 \leq n \leq 36 \\ -3 \times 10^{-2} \text{ mm} & \text{if } 37 \leq n \leq 48 \\ -1 \times 10^{-2} \text{ mm} & \text{if } 49 \leq n \leq 84 \\ 3 \times 10^{-2} \text{ mm} & \text{if } 85 \leq n \leq 96 \end{cases}$$

Figure: Ferreira, Marengo e Perego (2024).

Table: Physical properties for benchmark examples.

Example	E GPa	ν	G_c N/mm	ℓ_0 mm
L-Shaped	25.85	0.18	0.095	5.0

Source: Authors.

Figure: Specimen with load reversal.



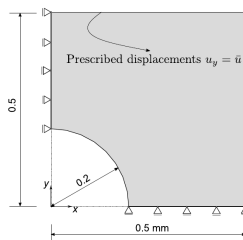
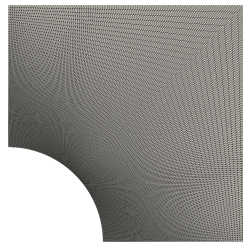
Figure: Reaction forces.

Source: Authors.

Source: Authors.

Holed Plate Specimen

Figure: Geometry and boundary conditions.



The imposed cyclic loading is specified as:

$$\Delta\bar{u}_n = \begin{cases} 1 \times 10^{-2} \text{ mm} & \text{if } 1 \leq n \leq 301 \\ 3 \times 10^{-2} \text{ mm} & \text{if } 302 \leq n \leq 903 \end{cases}$$

Figure: Ferreira, Marengo e Perego (2024).

Table: Physical properties for benchmark examples.

Example	E GPa	ν	G_c N/mm	ℓ_0 mm
Holed Plate	210	0.3	2.7	0.02

Source: Authors.

Figure: Specimen with load reversal.



Figure: Reaction forces.

Source: Authors.

Source: Authors.

Partial Conclusions

Results

The main contributions of this thesis are:

- Anisotropic phase-field damage formulation for elastic and fracture **anisotropy**.
- A parallel FEM code using **HPC** techniques and tools.
- Identification of model-implementation **limitations** and proposals for **extensions** (e.g., Drucker-Prager criteria and alternative energy splits).

The following key observations were made:

- The model closely **approximated the crack path and peak load** within the Vol-Dev model reference.
- The model **captured the load reversal** behavior accurately.
- The model is directly **extensible to anisotropic materials**.

Results

Despite the successful implementation and validation, some limitations remain:

- **Fixing H^- during staggered iterations.** In the current staggered solution strategy the negative Heaviside field H^- is held fixed until the minimum residual is reached, unlike the volumetric–deviatoric (Vol–Dev) split where H^- is allowed to evolve.
- **Energy split formulation and compressive fracture.** The present energy split does not represent fracture initiation under primarily compressive stress states. A possible remedy is to incorporate a Drucker–Prager type criterion.
- **Solver and scalability improvements.** While MPI provides good scalability, introducing better preconditioners and iterative solvers could further improve performance.

Next Steps

Next Steps

The next steps to be taken are:

- Validate the implementation of the transversely isotropic and orthotropic anisotropies of the constitutive tensor;
- Develop validation tests for transversely isotropic and orthotropic materials symmetries;
- Validate the implementation of the weak anisotropy model;
- Write an international paper for a high impact journal;
- Implement an efficient solver for the implemented strong anisotropy model;
- If possible: Development of at least one 3D example with trigonal symmetry.

References

ANAND, L.; GOVINDJEE, S. **Continuum Mechanics of Solids**. 1. ed. Oxford University PressOxford, 2020. ISBN 978-0-19-886472-1 978-0-19-189676-7. Disponível em: <<https://academic.oup.com/book/43650>>.

BHARALI, R. et al. A robust monolithic solver for phase-field fracture integrated with fracture energy based arc-length method and under-relaxation. **Computer Methods in Applied Mechanics and Engineering**, v. 394, p. 114927, maio 2022. ISSN 00457825. Disponível em: <<https://linkinghub.elsevier.com/retrieve/pii/S0045782522001992>>.

BONET, J.; GIL, A. J.; WOOD, R. D. **Nonlinear Solid Mechanics for Finite Element Analysis: Statics**. 1. ed. Cambridge University Press, 2016. ISBN 978-1-107-11579-8 978-1-316-33614-4. Disponível em: <<https://www.cambridge.org/core/product/identifier/9781316336144/type/book>>.

References (cont.)

- BOURDIN, B.; FRANC FORT, G.; MARIGO, J.-J. Numerical experiments in revisited brittle fracture. **Journal of the Mechanics and Physics of Solids**, v. 48, n. 4, p. 797–826, abr. 2000. ISSN 00225096. Disponível em: <doi:10.1016/S0022-5096(99)00028-9>.
- FERREIRA, A. R.; MAREN GO, A.; PEREGO, U. A phase-field gradient-based energy split for modeling of brittle fracture under cyclic loading. (**under revision**), 2024.
- FRANC FORT, G.; MARIGO, J.-J. Revisiting brittle fracture as an energy minimization problem. **Journal of the Mechanics and Physics of Solids**, v. 46, n. 8, p. 1319–1342, ago. 1998. ISSN 00225096. Disponível em: <doi:10.1016/S0022-5096(98)00034-9>.
- JONES, D. R. H.; ASHBY, M. F. **Engineering materials 1: an introduction to properties, applications and design**. Fifth edition. Oxford, United Kingdom: Butterworth-Heinemann, 2019. ISBN 978-0-08-102051-7.

References (cont.)

MARENGO, A. et al. A rigorous and efficient explicit algorithm for irreversibility enforcement in phase-field finite element modeling of brittle crack propagation. **Computer Methods in Applied Mechanics and Engineering**, p. 114137, dez. 2021. ISSN 00457825. Disponível em: <<https://linkinghub.elsevier.com/retrieve/pii/S0045782521004680>>.

MIEHE, C.; HOFACKER, M.; WELSCHINGER, F. A phase field model for rate-independent crack propagation: Robust algorithmic implementation based on operator splits. **Computer Methods in Applied Mechanics and Engineering**, v. 199, n. 45-48, p. 2765–2778, nov. 2010. ISSN 00457825. Disponível em: <[doi:10.1016/j.cma.2010.04.011](https://doi.org/10.1016/j.cma.2010.04.011)>.

Acknowledgments

Prof. Dr. Ayrton Ribeiro Ferreira (Advisor)

Prof. Dr. Marco Lúcio Bittencourt (External Examiner)

Prof. Dr. Rodolfo André Kuche Sanches (Internal Examiner)

Matt Knepley (PETSc Team)

CNPq - Conselho Nacional de Desenvolvimento Científico e Tecnológico

FAPESP - Fundação de Amparo à Pesquisa do Estado de São Paulo

*"Extraordinary claims require
extraordinary evidence."
— Carl Sagan*